Available online at www.sciencedirect.com

ScienceDirect

IFAC PapersOnline CONFERENCE PAPER ARCHIVE

IFAC PapersOnLine 51-29 (2018) 384–388

# Intent inference of ship maneuvering for automatic ship collision avoidance

**Yonghoon Cho, Jungwook Han, and Jinwhan Kim***

*Department of Mechanical Engineering, KAIST, Daejeon, Korea*
*(* corresponding author e-mail: jinwhan@kaist.ac.kr)*

**Abstract:**
This study addresses the intent inference of ship maneuvering with the consideration of the international regulations on marine traffic for preventing collisions at sea and its application to automatic ship collision avoidance. By assuming that the surrounding ship may or may not always follow the rules, the proposed method provides a decision-making procedure for safe navigation by predicting the maneuvering intent of traffic ships. A probabilistic approach based on a graphical model consisting of the maneuvering intent and evolution of system states is formulated and presented. To demonstrate and verify the feasibility of the proposed approach as an application of automatic ship collision avoidance, ship traffic simulations were conducted and the obtained results are provided and discussed.



*Keywords:* Intent inference, Ship collision avoidance, Graphical model

## 1. INTRODUCTION

For the safe operation of marine traffic ships, collision avoidance is an important capability because ship collisions may cause the loss of human life and extensive environmental damage. To prevent ship collisions, the international maritime organization (IMO) has published the international regulation for preventing collisions at sea (COLREGs) (Commandant, 1999), where the maritime traffic rules and the collision avoidance procedure are specified.

Previous studies on collision avoidance focused on the COLREGs-compliant path planning. Lee et al. (2004) developed a rule-compliant path planning algorithm, where the modified virtual force field (MVFF) and fuzzy-based algorithm were applied. Kuwata et al. (2014) modified the velocity obstacle (VO) with the worst case uncertainty (WVO), divided the velocity space into three parts and set one of the parts as a non-compliant action space. Among the graph search-based approaches, Campbell et al. (2012) introduced an A* based path planner that considers the regulations and Naeem et al. (2012) used the direction priority sequential selection (DPSS) and right-biased courses. The above studies assumed that the surrounding ships comply with the rule and/or maintain course and velocity. However, the surrounding ships may not always take compliant actions, which may lead to more dangerous encounter situations. Therefore, both compliant and non-compliant situations need to be considered for more reliable and robust collision avoidance. For this, the maneuver intentions of other ships should be estimated accurately and efficiently before initiating any collision avoidance actions.

In this paper, a novel approach to intent inference is proposed for automatic ship collision avoidance. The maneuver intentions of surrounding ships can be classified as either compliant or non-compliant based on the COLREGs. The probability of each intent is estimated within a graphical model framework, and the resulting equation is obtained based on Bayes' theorem and the concept of conditional independence. The feasibility of the proposed approach is validated through ship traffic simulations and the results are presented in this paper.

## 2. PROBLEM FORMULATION

In this study, when two surface ships approach each other, the ship under control is termed the "own ship," whereas the other ship is termed the "obstacle ship." Because the own ship directly reflects its intent onto the control, the maneuvering intent of the own ship can be known. However, knowing the intent of the obstacle ship is not straightforward. Therefore, the maneuvering intent of the obstacle ship is assumed to be unknown and have to be estimated from the observed action and its motion.

### 2.1 Intent inference

To calculate the maneuvering intent probability, a graphical model is constructed by combining the intentional behavior and the dynamic Bayesian network describing the evolution of control and state with feedback control (Thrun et al. (2005); Cho and Kim (2017)). Figure 1 describes the proposed graphical model. The intent model means that the intent takes an action and that action determines the state. The dynamic model represents the evolution of the state. Additionally, the state depends on the previous state and the current action, and the current action depends on the previous state caused by the feedback control scheme. If we assume that the action and state are known at time $k$, the maneuvering intent probability is expressed by Eq. (1).


10.1016/j.ifacol.2018.09.457

$$
\begin{aligned}
bel\Big(I_i(k)\Big) &= p\Big(I_i(k) \mid \mathbf{u}^k, \mathbf{x}^k\Big) \\
&= p\Big(I_i(k) \mid \mathbf{u}^{k-1}, \mathbf{x}^{k-1}, \mathbf{u}(k), \mathbf{x}(k)\Big) \\
&\overset{Bayes}{=} \eta p\Big(I_i(k) \mid \mathbf{u}^{k-1}, \mathbf{x}^{k-1}\Big) p\Big(\mathbf{u}(k), \mathbf{x}(k) \mid I_i(k), \mathbf{u}^{k-1}, \mathbf{x}^{k-1}\Big) \\
&\overset{Con.prob}{=} \eta p\Big(I_i(k) \mid \mathbf{u}^{k-1}, \mathbf{x}^{k-1}\Big) p\Big(\mathbf{x}(k) \mid I_i(k), \mathbf{u}^{k-1}, \mathbf{x}^{k-1}, \mathbf{u}(k)\Big) p\Big(\mathbf{u}(k) \mid I_i(k), \mathbf{u}^{k-1}, \mathbf{x}^{k-1}\Big) \\
&\overset{Con.indp}{=} \eta p\Big(I_i(k) \mid \mathbf{u}^{k-1}, \mathbf{x}^{k-1}\Big) p\Big(\mathbf{x}(k) \mid \mathbf{u}(k), \mathbf{x}(k-1)\Big) p\Big(\mathbf{u}(k) \mid I_i(k), \mathbf{x}(k-1)\Big) \\
&= \eta \sum_{j \in \{c,n\}} \Big[p\Big(I_i(k) \mid I_j(k-1)\Big) p\Big(I_j(k-1) \mid \mathbf{u}^{k-1}, \mathbf{x}^{k-1}\Big)\Big] p\Big(\mathbf{x}(k) \mid \mathbf{u}(k), \mathbf{x}(k-1)\Big) p\Big(\mathbf{u}(k) \mid I_i(k), \mathbf{x}(k-1)\Big)
\end{aligned} \tag{1}
$$

In Eq. (1), $I \in \{I_c, I_n\}$ is the union of the compliant intent $I_c$ and the non-compliant intent $I_n$. Because the intent cannot be chosen simultaneously, $I_c$ and $I_n$ are mutually exclusive. $I_i(k)$ is an element of the intent at time $k$. $bel\,(I_i(k))$ is the probability of $I_i$ at time k. $\mathbf{u}^k = \{\mathbf{u}(0), \cdots, \mathbf{u}(k)\}$, and $\mathbf{x}^k = \{\mathbf{x}(0), \cdots, \mathbf{x}(k)\}$ are the sets of all actions and states from the initial time to time $k$. $\eta$ is equal to $1/p\left(\mathbf{u}(k), \mathbf{x}(k) \mid \mathbf{u}^{k-1}, \mathbf{x}^{k-1}\right)$ and does not depend on $I_i(k)$. Thus, $\eta$ can be used as a normalizer (Thrun et al., 2005).

The concept of conditional independence is used to perform the calculation from the fourth to the fifth line in Eq. (1) (Bishop, 2006). $\mathbf{x}(k)$ is conditionally independent of $I_i(k)$, $\mathbf{u}^{k-1}$ and $\mathbf{x}^{k-2}$, given $\mathbf{u}(k)$ and $\mathbf{x}(k-1)$ in the proposed graphical model. The distribution of $\mathbf{x}(k)$ corresponding to the graphical model is expressed as follows:

$$
p\left(\mathbf{x}(k) \mid I_i(k), \mathbf{u}^{k-1}, \mathbf{x}^{k-1}, \mathbf{u}(k)\right) = p\left(\mathbf{x}(k) \mid \mathbf{u}(k), \mathbf{x}(k-1)\right). \tag{2}
$$

In the same manner, $\mathbf{u}(k)$ is conditionally independent of $\mathbf{u}^{k-1}$ and $\mathbf{x}^{k-2}$ given $I_i(k)$ and $x(k-1)$, and thus the distribution of $\mathbf{u}(k)$ can be expressed as follows:

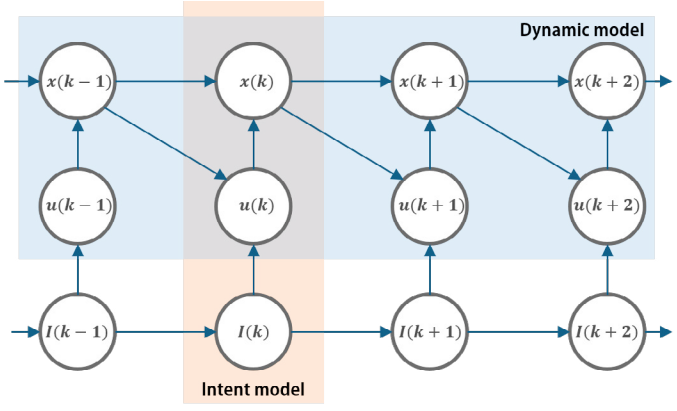


Fig. 1. Graphical model for maneuvering intent inference: The model is constructed by fusing the intent model and the dynamic model. The orange box represents the intent model and the blue box represents the dynamic model. $x$, $u$, $I$, and $k$ represent the relative state of the obstacle ship with respect to the own ship, action, intent, and time step, respectively.

$$
p\left(\mathbf{u}(k) \mid I_i(k), \mathbf{u}^{k-1}, \mathbf{x}^{k-1}\right) = p\left(\mathbf{u}(k) \mid I_i(k), \mathbf{x}(k-1)\right). \tag{3}
$$

The resultant equation consists of four equations. The intent transition probability $p\left(I_i(k) \mid I_j(k-1)\right)$ is the change probability from the previous to the next step. The intent transition probability is assumed to be known and time-invariant. Thus, the transition probability is predefined. $p\left(I_i(k) \mid \mathbf{u}^{k-1}, \mathbf{x}^{k-1}\right)$ is the maneuvering intent probability at the previous step. Each initial maneuvering intent probability is 0.5. The maneuvering intent at each time is calculated recursively from the initial probability. $p\left(\mathbf{x}(k) \mid \mathbf{u}(k), \mathbf{x}(k-1)\right)$ is the state transition probability.

$p\left(\mathbf{u}(k) \mid I_i(k), \mathbf{x}(k-1)\right)$ is the probability distribution of action at time $k$, which is modeled by using the instantaneous configuration between the own ship and the obstacle ship. Because compliant and non-compliant actions depend on the type of each encounter, the calculation method is different according to the type of encountered situation. The action is classified into three types: give-way, stand-on, and overtaking. When one ship approaches from the front and the starboard, the other ship have to alter its course to the starboard; this is classified as a give-way action. When one ship approaches from behind and the port, the other ship have to maintain its course and speed; this is classified as a stand-on action. When one ship is overtaken, the other ship keeps out of the way; this is classified as an overtaking action. Figure 2 is an illustration of the compliant and non-compliant region concept for each case. The regions in the give-way and overtaking cases are defined based on the VO concept of the velocity coordinates. Additionally, the regions in the stand-on case are defined in terms of maintaining the course and speed. If the obstacle ship takes a non-compliant action, the direction of action is expected to be inside of the non-compliant region. Therefore, the probability of action, given the intent and previous state, is expressed as follows:

$$
\begin{aligned}
p\left(\mathbf{u}(k) \mid I_c(k), \mathbf{x}(k-1)\right) &= \iint_{\mathcal{D}_c} f\left(\alpha \mathbf{u}(k), \mathbf{x}(k-1)\right) dA \\
p\left(\mathbf{u}(k) \mid I_n(k), \mathbf{x}(k-1)\right) &= \iint_{\mathcal{D}_n} f\left(\alpha \mathbf{u}(k), \mathbf{x}(k-1)\right) dA
\end{aligned} \tag{4}
$$

where $\mathcal{D}_c$ and $\mathcal{D}_n$ are the compliant and non-compliant regions defined in a two-dimensional space. $dA$ is an infinitesimal area. $f\left(\alpha \mathbf{u}(k), \mathbf{x}(k-1)\right)$ is the probability dis-

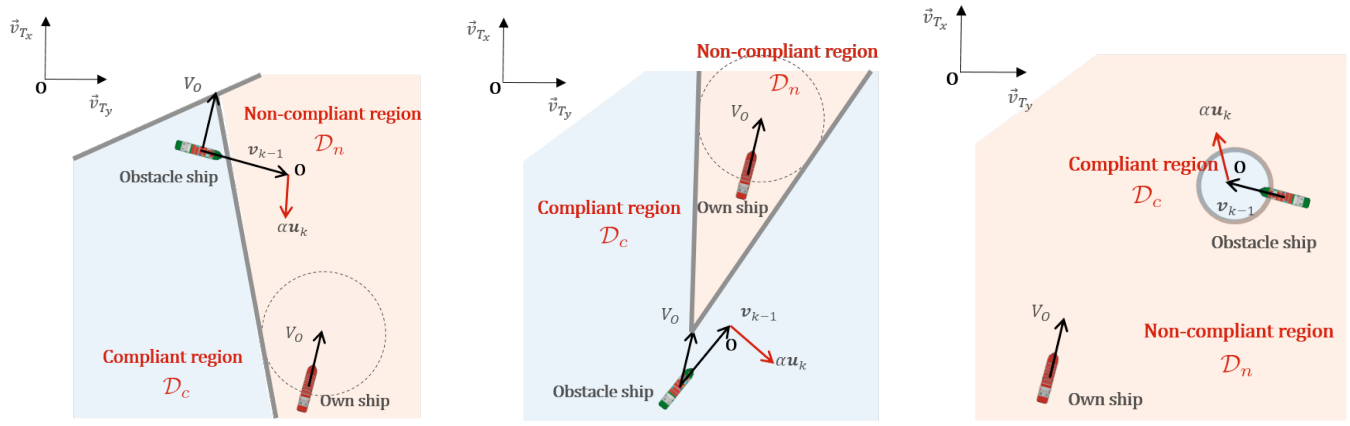


(a) Give-way (b) Overtaking (c) Stand-on

Fig. 2. Illustrations of compliant and non-compliant regions in three encounter situations: The red ship is the own ship and the green ship is the obstacle ship. $\mathbf{v}_{k-1}$ is the estimated velocity vector of the obstacle ship at time $k-1$. $\mathbf{u}_k$ is the estimated action vector at time $k$. $\alpha$ is the sensitivity parameter.

tribution of the action with respect to the previous state. The sensitivity parameter $\alpha$ adjusts the scale of the action in the velocity coordinate. As the sensitivity increases, the intent reacts to the action with more sensitivity.

### *2.2 Trajectory estimation*

With regard to the intent inference, target motion analysis and maneuvering estimation are implemented by using a two-stage Kalman filter (TSKF)-based tracking filter (Hsieh and Chen (1999); Alouani et al. (1991)). The TSKF consistes of a bias-free filter and a bias filter, whose structure is shown in Fig. 3. The bias-free filter estimates the system state without bias in the model, while the bias filter estimates the action. The coordinate system is shown in Fig. 4 and the state and action vectors are represented by

$$\begin{aligned}\mathbf{x} &= \begin{bmatrix} x_T & y_T & v_{Tx} & v_{Ty} \end{bmatrix}^\mathsf{T} \\ \mathbf{u} &= \begin{bmatrix} a_{Tx} & a_{Ty} \end{bmatrix}^\mathsf{T}\end{aligned} \tag{5}$$

where $\mathbf{v}_k \sim \mathcal{N}(0, \mathbf{R}_k)$ is the zero mean measurement noise in Cartesian coordinates.

where $x_T$ and $y_T$ represent the position of the obstacle ship. $v_{Tx}$ and $v_{Ty}$ represent the velocity in the $x$ and $y$ directions. $a_{Tx}$ and $a_{Ty}$ represent the acceleration in the $x$ and $y$ directions, respectively. $V_T = \sqrt{(v_{Tx}^2 + v_{Ty}^2)}$ and $\psi_T = \tan^{-1}(v_{Ty}/v_{Tx})$ are the linear velocity and the heading of the obstacle ship, respectively. The linear discrete stochastic system with an unknown action is expressed as follows:

$$\begin{aligned}\mathbf{x}_{k+1} &= \mathbf{A}_k \mathbf{x}_k + \mathbf{B}_k \mathbf{u}_{k+1} + \mathbf{w}_k^{\mathbf{x}} \\ \mathbf{u}_{k+1} &= \mathbf{u}_k + \mathbf{w}_k^{\mathbf{u}} \\ \mathbf{A}_k &= \begin{bmatrix} 1 & 0 & dt & 0 \\ 0 & 1 & 0 & dt \\ 0 & 0 & 1 & 0 \\ 0 & 0 & 0 & 1 \end{bmatrix}, \mathbf{B}_k = \begin{bmatrix} 0 & 0 \\ 0 & 0 \\ dt & 0 \\ 0 & dt \end{bmatrix}\end{aligned} \tag{6}$$

where $dt$ is the time-step interval. $\mathbf{w}_k^{\mathbf{x}} \sim \mathcal{N}(0, \mathbf{Q}_k^{\mathbf{x}})$, and $\mathbf{w}_k^{\mathbf{u}} \sim \mathcal{N}(0, \mathbf{Q}_k^{\mathbf{u}})$ are the zero mean Gaussian process noises. These noises reflect the uncertainty of the kinematic and action models, respectively. The measurement model is expressed as follows:

$$\begin{aligned}\mathbf{z}_k &= \mathbf{H}_k \mathbf{x}_k + \mathbf{v}_k \\ \mathbf{H}_k &= \begin{bmatrix} 1 & 0 & 0 & 0 \\ 0 & 1 & 0 & 0 \end{bmatrix}\end{aligned} \tag{7}$$

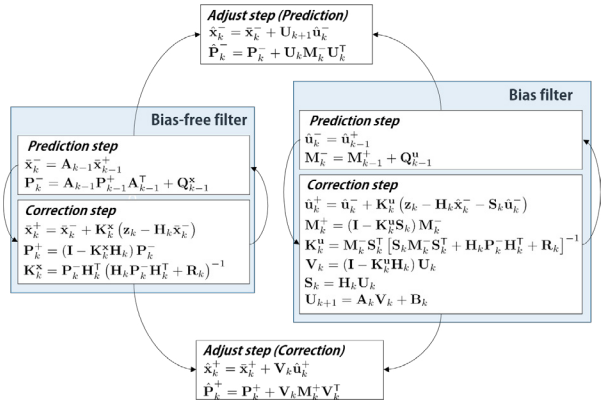


Fig. 3. TSKF structure consisting of a bias filter and a bias-free filter.

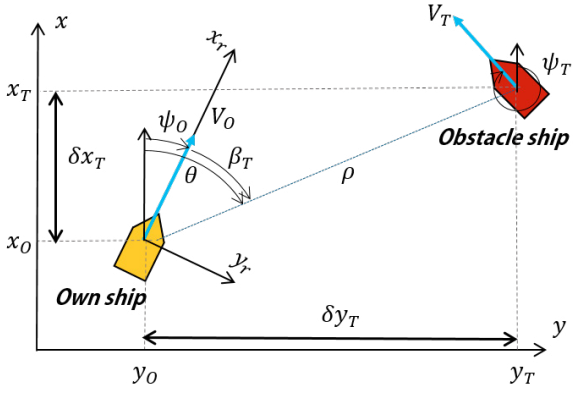


Fig. 4. Coordinate system between own ship and obstacle ship.

## 3. SIMULATION RESULT

Ship traffic simulations for two encounter cases are carried out to validate the feasibility of the proposed algorithm with the same initial simulation settings which are described in Table. 1. In the two simulations, it is assumed that the two ships on collision course cross each other. In the first scenario, the obstacle ship takes a compliant action. However, in the latter scenario, the obstacle ship does not take a compliant action.

Figure 5 shows the ship traffic simulation results. The upper figure shows the result when the obstacle ship follows the COLREGs, whereas the bottom figure shows the result when the obstacle ship violates the COLREGs. In each figure, the left sub-figure shows the ship trajectory, and the right sub-figure shows the estimated maneuver actions and intent probability. Here, the blue line represents the compliant maneuvering intent probability, and the red dotted line represents the non-compliant maneuvering intent probability. The violet dotted line represents the probability threshold. If the non-compliant maneuvering intent probability is continuously higher than the threshold probability for a specific period of time, the ship is regarded as violating the COLREGs. In the action estimation results, the green dotted line represents the estimated action, and the orange line represents the true acceleration. The results indicate that the estimated action and true acceleration are in good agreement.

In the first simulation case, the compliant maneuvering intent probability remains higher than the probability of non-compliant maneuvering intent because the obstacle ship takes a compliant action. Therefore, the own ship maintains its course and speed. However, in the second simulation, the obstacle ship maintains its course and speed against the COLREGs without taking any evasive action. Thus, the non-compliant maneuvering intent probability increases and becomes higher than the predefined threshold for more than the predefined period of time. Therefore, the own ship alters its course to the starboard side to avoid collision. After the course changes, the non-compliant intent decreases because the conflict has been resolved in the current configuration of the two ships.

Table 1. Ship traffic simulation settings

| **Parameter** | | **Value** |
|---|---|---|
| Length of ships | [m] | 175.00 |
| Breadth of ships | [m] | 25.40 |
| Minimum safe separation | [m] | 400 |
| Sensitivity parameter ($\alpha$) | | 10 |
| Transition matrix | $(i = j)$ | 0.65 |
| $p\left(I_i(k) \mid I_j(k-1)\right)$ | $(i \neq j)$ | 0.35 |
| Maneuvering intent threshold | | 0.6 |
| Initial position of own ship $(N, E)$ | [km] | (0, -5.0) |
| Initial position of obstacle ship $(N, E)$ | [km] | (5.0, 0) |
| Approaching speed $(V_{\mathrm{O}}, V_{\mathrm{T}})$ | [m/s] | (6, 6) |

## 4. CONCLUSION

In this paper, a novel method to estimate intent inference of an obstacle ship on collision course was proposed. A TSKF-based tracking filter was introduced to estimate both the action and the state of the obstacle ship. A graphical model was constructed with consideration of the state evolution with feedback control. Two cases of ship traffic simulations were conducted to validate the feasibility of the proposed approach and the obtained results were discussed.

## ACKNOWLEDGEMENTS

This research was part of the project titled "Development of a core technology and infra technology for the operation of USV with high reliability," which is funded by the ministry of Oceans and Fisheries, Korea, and was supported by the ICT R&D program of MSIP/IITP. [R-201500223-000167, Development of High Reliable Communications and Security SW for Various Unmanned Vehicles].

## REFERENCES

Alouani, A., Xia, P., Rice, T., and Blair, W. (1991). Two-stage kalman estimator for tracking maneuvering targets. In *Systems, Man, and Cybernetics, 1991.'Decision Aiding for Complex Systems, Conference Proceedings., 1991 IEEE International Conference on*, 761–766. IEEE.

Bishop, C. (2006). Pattern recognition and machine learning (information science and statistics), chapter 3, pages 138–147.

Campbell, S., Naeem, W., and Irwin, G.W. (2012). A review on improving the autonomy of unmanned surface vehicles through intelligent collision avoidance manoeuvres. *Annual Reviews in Control*, 36(2), 267–283.

Cho, Y. and Kim, J. (2017). Collision probability assessment between surface ships considering maneuver intentions. In *OCEANS 2017-Aberdeen*, 1–5. IEEE.

Commandant, U. (1999). International regulations for prevention of collisions at sea, 1972 (72 colregs). *US Department of Transportation, US Coast Guard, COMMANDANT INSTRUCTION M*, 16672.

Hsieh, C.S. and Chen, F.C. (1999). Optimal solution of the two-stage kalman estimator. *IEEE Transactions on automatic control*, 44(1), 194–199.

Kuwata, Y., Wolf, M.T., Zarzhitsky, D., and Huntsberger, T.L. (2014). Safe maritime autonomous navigation with colregs, using velocity obstacles. *IEEE Journal of Oceanic Engineering*, 39(1), 110–119.

Lee, S.M., Kwon, K.Y., and Joh, J. (2004). A fuzzy logic for autonomous navigation of marine vehicles satisfying colreg guidelines. *International Journal of Control, Automation, and Systems*, 2(2), 171–181.

Naeem, W., Irwin, G.W., and Yang, A. (2012). Colregs-based collision avoidance strategies for unmanned surface vehicles. *Mechatronics*, 22(6), 669–678.

Thrun, S., Burgard, W., and Fox, D. (2005). *Probabilistic robotics*. MIT press.

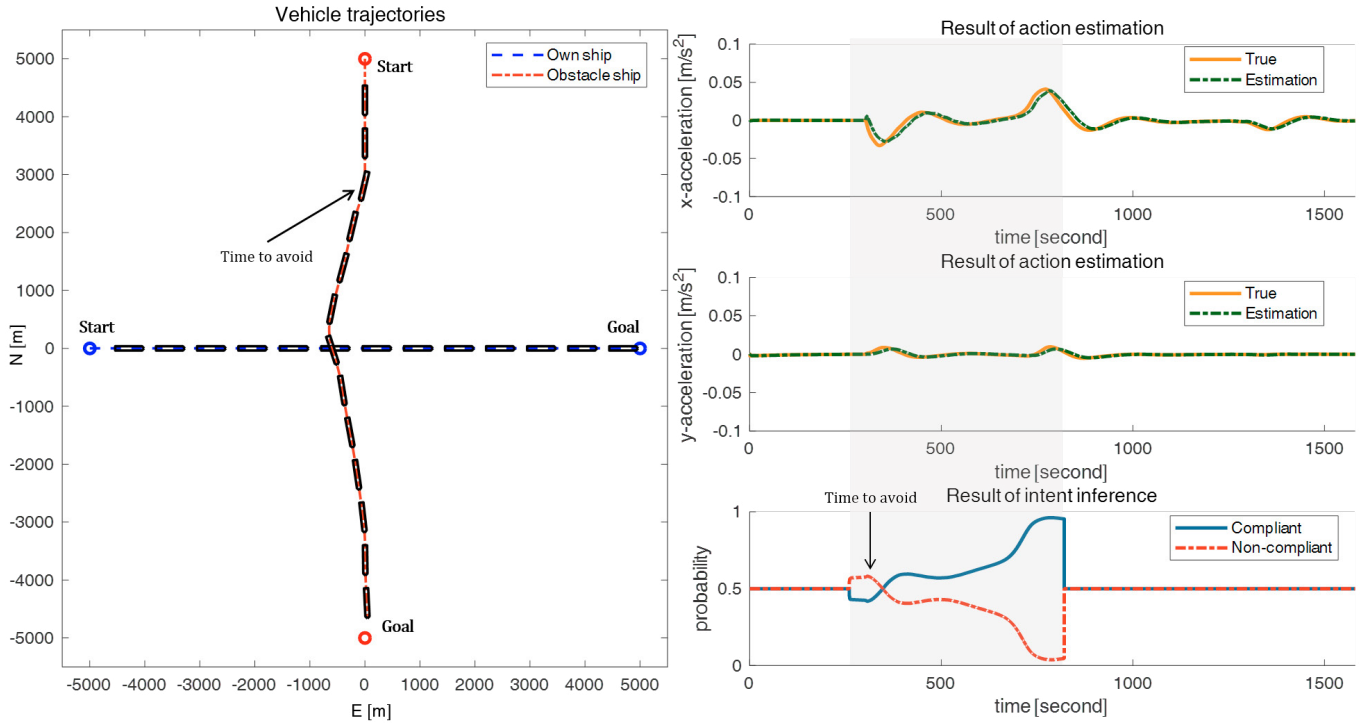


(a) Ship traffic simulation result: The own ship is a stand-on ship, and the obstacle ship is a give-way ship. The obstacle ship takes compliant evasive actions.

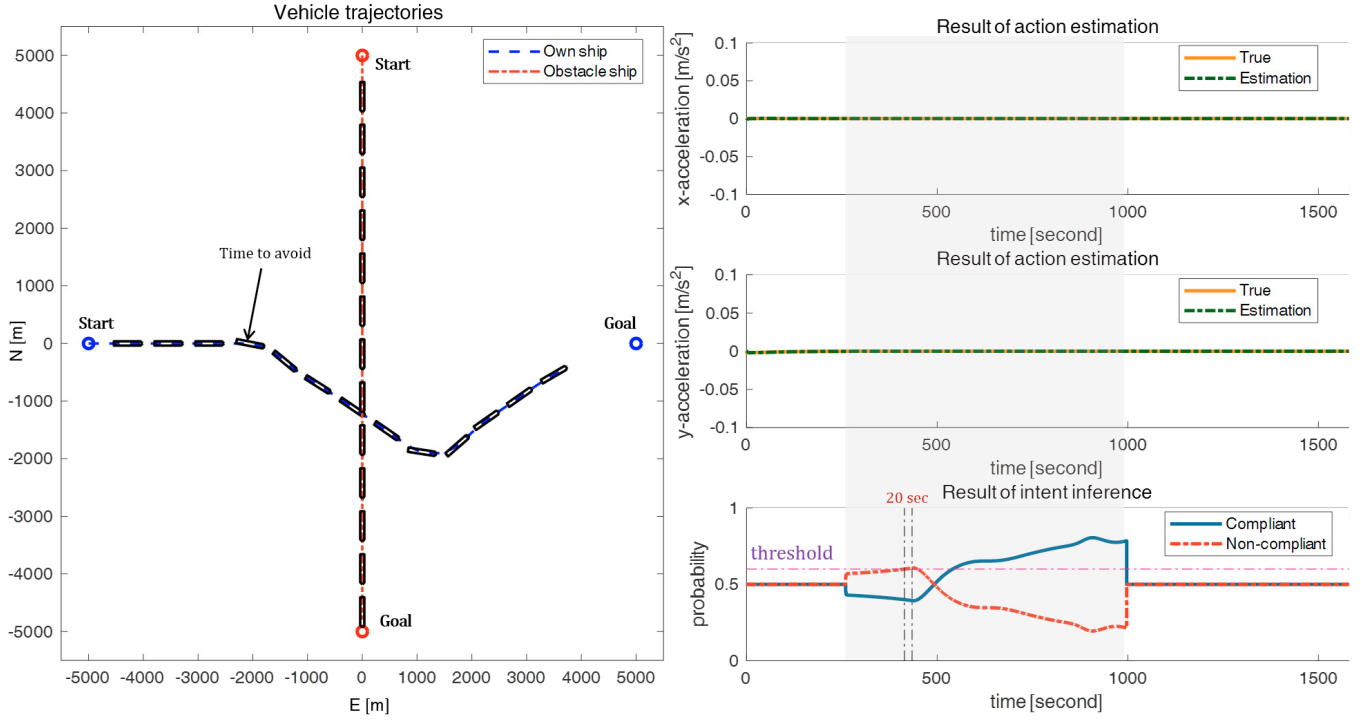


(b) Ship traffic simulation result: The own ship is a stand-on ship, and the obstacle ship is a give-way ship. The obstacle ship does not take any action.

Fig. 5. Comparison of ship traffic simulation results: The left figure in each case shows the trajectory of the two ships whose positions are plotted every two minutes. In each simulation case, the top-right and middle-right figures show the action estimation from the TSKF, and the bottom-right figure shows the result of intent inference. The shaded region in the right figures indicates the time range of inferring the maneuvering intent.